



Spinor Fourier Transform for Image Processing

Thomas Batard, Michel Berthier

► To cite this version:

| Thomas Batard, Michel Berthier. Spinor Fourier Transform for Image Processing. 2013. <hal-00807265>

HAL Id: hal-00807265

<https://hal.science/hal-00807265v1>

Preprint submitted on 3 Apr 2013

HAL is a multi-disciplinary open access archive for the deposit and dissemination of scientific research documents, whether they are published or not. The documents may come from teaching and research institutions in France or abroad, or from public or private research centers.

L'archive ouverte pluridisciplinaire **HAL**, est destinée au dépôt et à la diffusion de documents scientifiques de niveau recherche, publiés ou non, émanant des établissements d'enseignement et de recherche français ou étrangers, des laboratoires publics ou privés.



HAL Authorization

Spinor Fourier Transform for Image Processing

Thomas Batard, Michel Berthier

Abstract—We propose in this paper to introduce a new spinor Fourier transform for both grey-level and color image processing. Our approach relies on the three following considerations: mathematically speaking, defining a Fourier transform requires to deal with group actions; vectors of the acquisition space can be considered as generalized numbers when embedded in a Clifford algebra; the tangent space of the image surface appears to be a natural parameter of the transform we define by means of so-called spin characters. The resulting spinor Fourier transform may be used to perform frequency filtering that takes into account the Riemannian geometry of the image. We give examples of low-pass filtering interpreted as diffusion process. When applied to color images, the entire color information is involved in a really non marginal process.

Index Terms—Fourier transform, Scale-space, Riemannian geometry, Grey-level image, Color image.

I. INTRODUCTION

FROM the mathematical viewpoint, defining a Fourier transform requires the use of group representations (see Appendix B or [28]). Let us illustrate this fact on the well known shift theorem. If $f : \mathbb{R} \rightarrow \mathbb{R}$ is a function that admits a Fourier transform and $f_\alpha : \mathbb{R} \rightarrow \mathbb{R}$ is defined by

$$f_\alpha(x) = f(x + \alpha) \quad (1)$$

then the Fourier transforms $\mathcal{F}(f)$ and $\mathcal{F}(f_\alpha)$ of f and f_α are linked by

$$\mathcal{F}(f_\alpha)(u) = e^{2i\pi\alpha u} \mathcal{F}(f) \quad (2)$$

The group involved here is the additive group $(\mathbb{R}, +)$ of translations acting on \mathbb{R} by

$$(\alpha, x) \mapsto x + \alpha := \tau_\alpha(x) \quad (3)$$

The correspondence

$$\chi_u : \tau_\alpha \mapsto e^{2i\pi\alpha u} = \chi_u(\alpha) \quad (4)$$

is a composition law preserving map from the group $(\mathbb{R}, +)$ to the group \mathbb{S}^1 of unit complex numbers acting on \mathbb{C} by multiplication. It is a one-dimensional representation, *i.e.* a character, of the group $(\mathbb{R}, +)$. It appears that the Fourier transform is defined on the set of characters, also called the Pontryagin dual, by

$$\mathcal{F}(f)(u) = \int_{\mathbb{R}} f(x) \chi_u(-x) dx \quad (5)$$

identifying χ_u with u . The rest of this paper consists in showing how to generalize the above formula (5) so as to define a spinor Fourier transform well adapted to grey-level and color image processing.

Let us first formulate some remarks.

- 1) Marginal, *i.e.* componentwise, processing applied on color images is well known to produce false colors (see for instance [23] for examples of false colors). But it is not so clear when dealing with such images, how to define a Fourier transform which does not reduce to three Fourier transforms computed marginally and that takes into account color data.
- 2) The mathematical framework previously described also applies for a large range of groups. Considering the abelian finite group $\mathbb{Z}/N\mathbb{Z}$, resp. the abelian rotation group $SO(2, \mathbb{R})$, leads to the definition of the discrete Fourier transform, resp. the definition of the Fourier series. The non abelian case which requires more mathematical developments has been considered for instance in [27] to define generalized Fourier descriptors using the motion group of the plane and in [10] for the construction of so-called shearlets.
- 3) Very few works are devoted to a mixed approach of signal processing involving both harmonic and Riemannian methods. Although geometric decompositions such as curvelets take into account structure data (like edges), they are not directly defined by means of the Riemannian properties of the image surface.
- 4) As we are mainly concerned by grey-level and color image processing, it is important to note that the spinor Fourier transform we want to define must be computed with usual complex fast Fourier transforms.

Let us now describe the main underlying key ideas of this work. The first one is to extend the usual approach mentioned above to n -dimensional images by replacing the involved complex characters by characters with values in a group acting on the acquisition n -dimensional vector space. One way to proceed is to treat vectors as generalized numbers. This can be done by embedding the acquisition space in an algebra where are defined the four usual operations $(+, -, \times, /)$ (the inverse is defined only for invertible elements). As examples, it is well known that vectors of \mathbb{R}^2 , resp. vectors of \mathbb{R}^4 , can be identified with complex, resp. hypercomplex (quaternion) numbers (in both cases all non zero elements are invertible). We propose here to deal with Clifford algebras of which the complex and quaternion algebras appear to be particular cases. These algebras have already been used in many works related to signal processing (see [17], [14], [3], [2] or [13] for instance). We are led to consider spin characters, that is composition law preserving maps from the group $(\mathbb{R}^2, +)$ with values in spin groups. These latter act on vector spaces through the standard representations

$$\rho_n : Spin(n) \rightarrow SO(n, \mathbb{R}) \quad (6)$$

that describe the groups $Spin(n)$ as double-sheeted coverings of the orthogonal groups $SO(n, \mathbb{R})$ (see [25]). By averaging

this action we define a Clifford Fourier transform which appears to generalize in a very natural way the formula (5).

The second idea is to involve explicitly the geometry of the image surface that is embedded for instance in \mathbb{R}^3 , resp. \mathbb{R}^5 when considering grey-level, resp. color images. The already mentioned spin characters are parametrized by so-called bivectors (see [20]). Very roughly speaking these bivectors, which are elements of the Clifford algebra, encode planes of \mathbb{R}^3 or \mathbb{R}^5 . By using bivectors corresponding to the tangent planes of the image surface, one can parametrize the Clifford Fourier transform so as to take into account the Riemannian geometry of the image surface. To set up this idea one has to consider images as sections of associated vector bundles built from the standard representations of spin groups (see [18]). These bundles are called spinor bundles and the corresponding sections spinor fields.

Finally, we introduce a Riemannian harmonic decomposition for images. The usual 2D discrete Fourier transform provides a basis of decomposition for say grey-level images given by

$$(m, n) \mapsto e^{2i\pi(um/M + vn/N)} \quad (7)$$

with $u \in \mathbb{Z}/M\mathbb{Z}$ and $v \in \mathbb{Z}/N\mathbb{Z}$, in such a way that any image f of size $M \times N$ can be written as

$$f(m, n) = \sum \hat{f}(u, v) e^{2i\pi(um/M + vn/N)} \quad (8)$$

the sum running over $m \in \mathbb{Z}/M\mathbb{Z}$ and $n \in \mathbb{Z}/N\mathbb{Z}$. The main drawbacks of this basis are that this one neither involves local geometric data nor extends in a non marginal way to multi-channel images. Using the spinor Fourier transform and the Riemannian settings described above allows one to obtain a decomposition basis for the image surface which takes into account both local geometric and color information. To illustrate this approach, we perform frequency filterings and show applications on well known images.

Let us mention that in this paper we consider the only standard representations (6) of the spin groups. Other representations exist beside these which are called spin representations and that come from the complex representations of Clifford algebras. These representations do not descend to orthogonal groups (see [21]). The study of the corresponding Riemannian harmonic decomposition will appear elsewhere.

II. CLIFFORD FOURIER TRANSFORMS

THERE have been many attempts to generalize the usual Fourier transform in the framework of quaternion or Clifford algebras. We mention here briefly some of the already existing definitions and describe the construction involving the spin characters. The reader will find in the appendices the mathematical definitions and results used here.

A. Quaternionic and Clifford Fourier transforms

The quaternionic transform introduced in [26] (see also [15]) reads

$$\mathcal{F}_\mu f(U) = \int_{\mathbb{R}^2} f(X) \exp(-\mu \langle X, U \rangle) dX \quad (9)$$

$X = (x_1, x_2)$, $U = (u_1, u_2)$, and is defined for a function (color image) $f : \mathbb{R}^2 \rightarrow \mathbb{H}_0$, where \mathbb{H}_0 is the set of imaginary quaternions. The unit imaginary quaternion μ is chosen to be $\mu = (i + j + k)/\sqrt{3}$ (representing the grey axis) and satisfies $\mu^2 = -1$. The corresponding quaternionic Fourier coefficients are decomposed with respect to a symplectic split associated to μ , each one of the factors being expressed in the polar form:

$$\mathcal{F}_\mu f = A_\parallel \exp[\mu \theta_\parallel] + A_\perp \exp[\mu \theta_\perp] \nu \quad (10)$$

with ν an imaginary unit quaternion orthogonal to μ . The authors propose a spectral interpretation from this decomposition (see [26] for details).

In [7] (see also [8]) the approach is quite different since it concerns mainly the analysis of symmetries of a signal f from \mathbb{R}^2 to \mathbb{R} given for example by a grey-level image. For such a signal, the quaternionic Fourier transform introduced in [7] reads:

$$\mathcal{F}_{ij} f(U) = \int_{\mathbb{R}^2} \exp(-2\pi i u_1 x_1) f(X) \exp(-2\pi j u_2 x_2) dX \quad (11)$$

Note that i and j can be replaced by arbitrary pure imaginary quaternions. The choice of this formula is justified by the following equality:

$$\mathcal{F}_{ij} f(U) = \mathcal{F}_{cc} f(U) - i \mathcal{F}_{sc} f(U) - j \mathcal{F}_{cs} f(U) + k \mathcal{F}_{ss} f(U) \quad (12)$$

where

$$\mathcal{F}_{cc} f(U) = \int_{\mathbb{R}^2} f(X) \cos(2\pi u_1 x_1) \cos(2\pi u_2 x_2) dX \quad (13)$$

and similar expressions involving sines and cosines for $\mathcal{F}_{sc} f$, $\mathcal{F}_{cs} f$ and $\mathcal{F}_{ss} f$.

It is important to note at this stage that the kernels used in (9) and (11) correspond to rotations in the space \mathbb{R}^4 under the identification of the group $Spin(4)$ with the group $\mathbb{H}^1 \times \mathbb{H}^1$ where \mathbb{H}^1 is the group of unit quaternions (see Appendix A or [22]).

In [16], the Clifford Fourier transform is defined by

$$\mathcal{F}_{e_1 e_2} f(U) = \int_{\mathbb{R}} \exp(-2\pi e_1 e_2 \langle U, X \rangle) f(X) dX \quad (14)$$

for a function $f(X) = f(x) e_2$ from \mathbb{R} to \mathbb{R} and by

$$\mathcal{F}_{e_1 e_2 e_3} f(U) = \int_{\mathbb{R}^2} \exp(-2\pi e_1 e_2 e_3 \langle U, X \rangle) f(X) dX \quad (15)$$

for a function $f(X) = f(x_1, x_2) e_3$ from \mathbb{R}^2 to \mathbb{R} . The element $e_1 e_2$, resp. $e_1 e_2 e_3$, is the so-called pseudoscalar of the Clifford algebra $\mathbb{R}_{2,0}$, resp. $\mathbb{R}_{3,0}$. These transforms appear naturally when dealing with the analytic and monogenic signals.

The definition of [14] also uses the kernel of (15). If f is a function from \mathbb{R}^3 to the Clifford algebra $\mathbb{R}_{3,0}$, then

$$\mathcal{F}_{e_1 e_2 e_3} f(U) = \int_{\mathbb{R}^3} f(X) \exp(-2\pi e_1 e_2 e_3 \langle U, X \rangle) dX \quad (16)$$

Note that if we set

$$\begin{aligned} f &= f_0 + f_1 e_1 + f_2 e_2 + f_3 e_3 + \\ &f_{23} i_3 e_1 + f_{31} i_3 e_2 + f_{12} i_3 e_3 + f_{123} i_3 \end{aligned} \quad (17)$$

with $i_3 = e_1 e_2 e_3$, this transform can be written as a sum of four complex Fourier transforms by identifying i_3 with the imaginary complex i . In particular, for a function f with values in the vector part of the Clifford algebra, this reduces to marginal, *i.e.* componentwise, processing. This Clifford Fourier transform is used to analyze frequencies of vector fields and the behavior of vector valued filters.

The definition proposed in [3] relies on Clifford analysis and involves the so-called angular Dirac operator Γ . The general formula is

$$\mathcal{F}_\pm f(U) = \left(\frac{1}{\sqrt{2\pi}} \right)^n \int_{\mathbb{R}^n} \exp(\mp i \frac{\pi}{2} \Gamma_U) \times \exp(-i \langle U, X \rangle) f(X) dX \quad (18)$$

For the special case of a function f from \mathbb{R}^2 to $\mathbb{C}_2 = \mathbb{R}_{0,2} \otimes \mathbb{C}$, the transform reads

$$\mathcal{F}_\pm f(U) = \frac{1}{2\pi} \int_{\mathbb{R}^2} \exp(\pm U \wedge X) f(X) dX \quad (19)$$

Let us remark that $\exp(\pm U \wedge X)$ is the exponential of a bivector, *i.e.* a spinor. This construction allows to introduce two dimensional Clifford Gabor filters.

Let us mention that the above transform (19) is a very special case of a more general transform defined by means of Clifford analysis. We refer the reader to [4], [11] and [12] for details. Finally, alternative definitions can be found in [5] and [6] based on Clifford generalizations of the squared root of -1.

B. Clifford Fourier transform with spin characters

The transform defined in [1] is based on a spin generalization of the usual notion of group characters (see Sec. III.C). If f is a function from \mathbb{R}^2 with values in the vector part of the Clifford algebra $\mathbb{R}_{4,0}$ then

$$\mathcal{CF}f(u_1, u_2, u_3, u_4, D) =$$

$$\int_{\mathbb{R}^2} f(x_1, x_2) \perp \varphi_{(u_1, u_2, u_3, u_4, D)}(-x_1, -x_2) dx_1 dx_2 \quad (20)$$

with

$$(x_1, x_2) \mapsto \varphi_{(u_1, u_2, u_3, u_4, D)}(x_1, x_2) \quad (21)$$

the spin character that sends (x_1, x_2) to the product

$$\begin{aligned} & \exp \left[\frac{1}{2} [x_1(u_1 + u_3) + x_2(u_2 + u_4)] D \right] \\ & \times \exp \left[\frac{1}{2} [x_1(u_1 - u_3) + x_2(u_2 - u_4)] I_4 D \right] \end{aligned} \quad (22)$$

where D is a unit bivector of $\mathbb{R}_{4,0}$, I_4 is the pseudo scalar and \perp is the action of $Spin(4)$ on \mathbb{R}^4 (see Appendix A). For the special case of a color image

$$f : (x_1, x_2) \mapsto f_1(x_1, x_2)e_1 + f_2(x_1, x_2)e_2 + f_3(x_1, x_2)e_3 \quad (23)$$

the Clifford Fourier transform of the function f in the direction D is given by

$$\begin{aligned} & \mathcal{CF}_D f(u_1, u_2) = \\ & \int_{\mathbb{R}^2} f(x_1, x_2) \perp \varphi_{(u_1, u_2, 0, 0, D)}(-x_1, -x_2) dx_1 dx_2 \end{aligned} \quad (24)$$

Note that formulas (20) and (24) appear as natural generalizations of the usual 2D Fourier transform for an \mathbb{R} -valued function written as

$$\mathcal{F}f(u_1, u_2) =$$

$$\int_{\mathbb{R}^2} f(x_1, x_2) \perp \varphi_{(u_1, u_2, e_1 e_2)}(-x_1, -x_2) dx_1 dx_2 \quad (25)$$

where

$$f(x_1, x_2) = f_1(x_1, x_2)e_1 + f_2(x_1, x_2)e_2 \quad (26)$$

and

$$\varphi_{(u_1, u_2, e_1 e_2)}(x_1, x_2) = \exp \left[\frac{1}{2} (x_1 u_1 + x_2 u_2) e_1 e_2 \right] \quad (27)$$

(compare with equation (5)). In (24) the two frequencies u_3 and u_4 are chosen to be zero, this corresponds to the fact that the involved rotations in \mathbb{R}^4 are isocline (see [22]).

Applications to color image processing are described in [1]. See also [24] for the construction of generalized color Fourier descriptors.

The main drawback of this transform is that it is a global transform with a fixed parametrizing bivector that does not take into account the geometric data.

III. THE GEOMETRICAL FRAMEWORK

TO tackle this problem, we propose in this section to introduce a geometrical framework which allows for a pointwise version of the above transform. We refer the reader to [18] and [21] for the mathematical definitions and results used in particular in Sec. III. B.

A. From functions to surfaces

Let

$$f : (x_1, x_2) \in \Omega \mapsto f(x_1, x_2) \quad (28)$$

be a grey-level image defined on a domain Ω of \mathbb{R}^2 . Such an image can be considered as a surface Σ embedded in \mathbb{R}^3 by the parametrization

$$\varphi : (x_1, x_2) \mapsto (x_1, x_2, f(x_1, x_2)) \quad (29)$$

that is as a 2-dimensional Riemannian surface with a global chart (Ω, φ) . The Riemannian metric on Σ is the one induced by the Euclidean metric of \mathbb{R}^3 .

Looking at formula (24) it seems natural to try to replace the parametrizing bivector mentioned above by a unit bivector field coding the tangent planes to Σ . This is the simplest way to involve the geometry of Σ . But there are now two problems to deal with.

- 1) This bivector field (of the Clifford algebra $\mathbb{R}_{3,0}$) is clearly no longer constant.
- 2) To define the \perp action in this context, one has to introduce a varying space of representation.

In the same way, if

$$f : (x_1, x_2) \in \Omega \mapsto (f_1(x_1, x_2), f_2(x_1, x_2), f_3(x_1, x_2)) \quad (30)$$

is a color image, it can be considered as a surface Σ embedded in \mathbb{R}^5 by the parametrization

$$\varphi : (x_1, x_2) \mapsto (x_1, x_2, (f_1(x_1, x_2), f_2(x_1, x_2), f_3(x_1, x_2))) \quad (31)$$

and in this case one has to deal with varying bivectors of the Clifford algebra $\mathbb{R}_{5,0}$.

Solving the problems listed above requires the introduction of some advanced mathematical concepts (such as spinor bundles). The reader not familiar with these concepts can skip this part of the paper since we explain later how to compute practically the new defined spinor Fourier transform. Let us just mention that because of the desire to use complex fast Fourier transforms we are led to consider surfaces as embedded in \mathbb{R}^4 for grey-level images and in \mathbb{R}^6 for color images.

B. Images as sections of associated bundles

Let Ω be an open set of \mathbb{R}^2 (the domain of the image). Let $P_{SO}(E_n(\Omega))$ be the principal $SO(n, \mathbb{R})$ -bundle of oriented frames of the trivial bundle $E_n(\Omega) = \Omega \times \mathbb{R}^n$. A spin structure on $E_n(\Omega)$ is a principal $Spin(n)$ -bundle, denoted $P_{Spin}(E_n(\Omega))$, together with a 2-sheeted covering

$$P_{Spin}(E_n(\Omega)) \longrightarrow P_{SO}(E_n(\Omega)) \quad (32)$$

that is compatible with $SO(n, \mathbb{R})$ and $Spin(n)$ actions. We consider the following action

$$Spin(n) \times P_{Spin}(E_n(\Omega)) \times \mathbb{R}^n \longrightarrow P_{Spin}(E_n(\Omega)) \times \mathbb{R}^n \quad (33)$$

given by

$$(\tau, p, z) \longmapsto (p\tau^{-1}, \rho_n(\tau)z) \quad (34)$$

where

$$\rho_n : Spin(n) \longrightarrow SO(n, \mathbb{R}) \quad (35)$$

is the standard representation of the group $Spin(n)$ (see Appendix A). The associated bundle $P_{Spin}(E_n(\Omega)) \times_{\rho_n} \mathbb{R}^n$ is the quotient of the product $P_{Spin}(E_n(\Omega)) \times \mathbb{R}^n$ by the action (33). It is a vector bundle over Ω with fiber \mathbb{R}^n .

Let now

$$f : (x_1, x_2) \in \Omega \longmapsto f(x_1, x_2) \quad (36)$$

be a grey-level image. Such an image is considered as a section of the associated bundle $P_{Spin}(E_4(\Omega)) \times_{\rho_4} \mathbb{R}^4$, that is as a map

$$\sigma : \Omega \longrightarrow P_{Spin}(E_4(\Omega)) \times_{\rho_4} \mathbb{R}^4 \quad (37)$$

such that

$$\pi_4 \circ \sigma = Id \quad (38)$$

where

$$\pi_4 : P_{Spin}(E_4(\Omega)) \times_{\rho_4} \mathbb{R}^4 \longrightarrow \Omega \quad (39)$$

is the vector bundle projection. This section is given by

$$\sigma(x_1, x_2) = f(x_1, x_2)e_3 \quad (40)$$

In the same way, to a color image

$$f : (x_1, x_2) \in \Omega \longmapsto (f_1(x_1, x_2), f_2(x_1, x_2), f_3(x_1, x_2)) \quad (41)$$

corresponds the section

$$\sigma(x_1, x_2) = f_1(x_1, x_2)e_3 + f_2(x_1, x_2)e_4 + f_3(x_1, x_2)e_5 \quad (42)$$

of the associated vector bundle $P_{Spin}(E_6(\Omega)) \times_{\rho_6} \mathbb{R}^6$. At a given point (x_1, x_2) of Ω the value of the section σ belongs to a representation space on which the spin group consider as the fiber of $P_{Spin}(E_n(\Omega))$ at (x_1, x_2) acts. This allows to define a new spinor Fourier transform.

Remark. This geometric description applies for n -dimensional images, $n \geq 3$. As we will see later, the necessity of splitting the new defined transform onto orthogonal planes to apply complex fast Fourier transforms, impose here to treat the cases $n = 4$ and $n = 6$.

C. Spin characters and tangent planes

Let us first describe the spin characters involved (through the sections of the bundle $P_{Spin}(E_n(\Omega))$ in the definition of the spinor Fourier transform (see [1] for an alternative approach of the proofs).

Theorem 1: The morphisms from the additive group \mathbb{R}^2 to the spin group $Spin(4)$ (the $Spin(4)$ characters) are given by

$$(x_1, x_2) \longmapsto \exp \frac{1}{2} \left[(B_1 \ B_2) A \begin{pmatrix} x_1 \\ x_2 \end{pmatrix} \right] \quad (43)$$

where A is a 2×2 real matrix (the frequency matrix) and

$$B_i = e_i f_i \quad (44)$$

for $i = 1, 2$, with (e_1, e_2, f_1, f_2) an orthonormal basis of \mathbb{R}^4 .

Proof: it relies on the following arguments.

- 1) \mathbb{R}^2 is simply connected so that every Lie group morphism from \mathbb{R}^2 to $Spin(4)$ is given by the exponentiation of a Lie algebra homomorphism from \mathbb{R}^2 to the Lie algebra $\mathfrak{spin}(4)$ of $Spin(4)$.
- 2) The group $Spin(4)$ is isomorphic to the group product $Spin(3) \times Spin(3)$.
- 3) The abelian Lie subalgebras of the Lie algebra $\mathfrak{spin}(3)$ of the group $Spin(3)$ are of dimension 1.
- 4) The orthogonalization algorithm of Hestenes on bivectors (see [20]) allows to express the morphisms from \mathbb{R}^2 to $Spin(3) \times Spin(3)$ as in formula (44).

A $Spin(4)$ character is then parametrized by 4 real numbers (the frequencies) and an orthonormal basis of \mathbb{R}^4 .

Theorem 2: The morphisms from the additive group \mathbb{R}^2 to the spin group $Spin(6)$ (the $Spin(6)$ characters) are given by

$$(x_1, x_2) \longmapsto \exp \frac{1}{2} \left[(B_1 \ B_2 \ B_3) A \begin{pmatrix} x_1 \\ x_2 \end{pmatrix} \right] \quad (45)$$

where A is a 3×2 real matrix (the frequency matrix) and

$$B_i = e_i f_i \quad (46)$$

for $i = 1, 2, 3$, with $(e_1, e_2, e_3, f_1, f_2, f_3)$ an orthonormal basis of \mathbb{R}^6 .

Proof: as in the proof of Theorem 1, we have to describe the Lie algebra homomorphisms from \mathbb{R}^2 to the Lie algebra $\mathfrak{spin}(6)$ of the group $Spin(6)$. This is done using the following results:

1) $Spin(6)$ is isomorphic to $SU(4)$: consider

$$Spin(6) \subset \mathbb{R}_{6,0}^{(0)} \simeq \mathbb{R}_{5,0} \simeq \mathbb{C}(4) \quad (47)$$

so that $Spin(6)$ appears as a subgroup of $GL(4, \mathbb{C})$ which implies by standard arguments (compactness and connectedness) the isomorphism.

- 2) As a consequence, the Lie algebra $\mathfrak{spin}(6)$ of $Spin(6)$ is of type $E(3)$ so that it contains maximal abelian Lie subalgebras of dimension 3.
- 3) The bivectors B_i form bases of such Lie sub-algebras (Cartan subalgebras). ■

A $Spin(6)$ character is then parametrized by 6 real numbers (the frequencies) and an orthonormal basis of \mathbb{R}^6 .

In the rest of this paper, the spin characters (43) and (45) are denoted $\chi_{A,B}$ (A is the involved frequency matrix and B stands for (B_1, B_2) or (B_1, B_2, B_3) depending on the context). Considering images as sections of the bundle $P_{Spin}(E_n(\Omega)) \times_{\rho_n} \mathbb{R}^n$ ($n = 4$ or $n = 6$) allows to deal with actions of sections of the bundle $P_{Spin}(E_n(\Omega))$. This means that B is no longer fixed and may depend of the current point.

Let now

$$\varphi : (x_1, x_2) \mapsto (x_1, x_2, f(x_1, x_2)) \quad (48)$$

be the graph of a grey-level image. At each point p of Ω , the space \mathbb{R}^3 splits into

$$\mathbb{R}^3 = T_{\varphi(p)}\Sigma \oplus N_{\varphi(p)}\Sigma \quad (49)$$

where T_Σ , resp. N_Σ , denotes the tangent, resp. the normal, bundle of the surface Σ . Let F_4 be the bundle

$$F_4 = T_\Sigma \oplus N_\Sigma \oplus \mathbb{R}e_4 \quad (50)$$

and $Cl(F_4)$ be the corresponding Clifford bundle. The degree one sections of $Cl(F_4)$ can be identified with functions from Ω to \mathbb{R}^4 and as mentioned before, we consider the image as a section $\sigma(x_1, x_2) = f(x_1, x_2)e_3$ of $Cl(F_4)$. The tangent bundle $T\Sigma$ is encoded by the degree 2 section (the bivector field)

$$B_1 = \frac{\varphi_{x_1} \wedge \varphi_{x_2}}{\|\varphi_{x_1} \wedge \varphi_{x_2}\|} \quad (51)$$

of $Cl(F_4)$. Here φ_{x_i} denotes the partial derivative of φ with respect to x_i . More precisely,

$$B_1 = \gamma_1 e_1 e_2 + \gamma_2 e_1 e_3 + \gamma_3 e_2 e_3 \quad (52)$$

where

$$\gamma_1 = \frac{1}{\sqrt{1 + f_{x_1}^2 + f_{x_2}^2}} \quad \gamma_2 = \frac{f_{x_2}}{\sqrt{1 + f_{x_1}^2 + f_{x_2}^2}} \quad (53)$$

and

$$\gamma_3 = \frac{-f_{x_1}}{\sqrt{1 + f_{x_1}^2 + f_{x_2}^2}} \quad (54)$$

In this case B_2 is given by $I_4 B_1$ (I_4 is the pseudo scalar of the Clifford algebra $\mathbb{R}_{4,0}$), that is

$$B_2 = -\gamma_3 e_1 e_4 + \gamma_2 e_2 e_4 - \gamma_1 e_3 e_4 \quad (55)$$

In the same way, if

$$\varphi : (x_1, x_2) \mapsto (x_1, x_2, f_1(x_1, x_2), f_2(x_1, x_2), f_3(x_1, x_2)) \quad (56)$$

is the graph of a color image, we introduce the decomposition

$$\mathbb{R}^5 = T_{\varphi(p)}\Sigma \oplus N_{\varphi(p)}\Sigma \quad (57)$$

the bundle

$$F_6 = T_\Sigma \oplus N_\Sigma \oplus \mathbb{R}e_6 \quad (58)$$

the Clifford bundle $Cl(F_6)$ and identify a color image with a degree one section $\sigma(x_1, x_2) = f_1(x_1, x_2)e_3 + f_2(x_1, x_2)e_4 + f_3(x_1, x_2)e_5$ of $Cl(F_6)$. In this case the bivector B_1 reads

$$B_1 = \gamma_1 e_1 e_2 + \gamma_2 e_1 e_3 + \gamma_3 e_1 e_4 + \gamma_4 e_1 e_5 + \gamma_5 e_2 e_3 + \gamma_6 e_2 e_4 + \gamma_7 e_2 e_5 + \gamma_8 e_3 e_4 + \gamma_9 e_3 e_5 + \gamma_{10} e_4 e_5 \quad (59)$$

where

$$\begin{aligned} \gamma_1 &= 1/\delta \quad \gamma_2 = (f_1)_{x_2}/\delta \quad \gamma_3 = (f_2)_{x_2}/\delta \quad \gamma_4 = (f_3)_{x_2}/\delta \\ \gamma_5 &= (-f_1)_{x_1}/\delta \quad \gamma_6 = (-f_2)_{x_1}/\delta \quad \gamma_7 = (-f_3)_{x_1}/\delta \\ \gamma_8 &= [(f_1)_{x_1}(f_2)_{x_2} - (f_1)_{x_2}(f_2)_{x_1}]/\delta \\ \gamma_9 &= [(f_1)_{x_1}(f_3)_{x_2} - (f_1)_{x_2}(f_3)_{x_1}]/\delta \\ \gamma_{10} &= [(f_2)_{x_1}(f_3)_{x_2} - (f_2)_{x_2}(f_3)_{x_1}]/\delta \end{aligned} \quad (60)$$

with $\delta = \|\varphi_{x_1} \wedge \varphi_{x_2}\|$. The bivectors B_2 and B_3 are determined using Gram-Schmidt algorithm (see remark 3 below).

D. The spinor Fourier transform

We follow the same procedure as in Sec. II.B. Let σ be a section of the bundle $P_{Spin}(E_n(\Omega)) \times_{\rho_n} \mathbb{R}^n$ ($n = 4$ or $n = 6$) and $\chi_{A,B}$ be a section of $P_{Spin}(E_n(\Omega))$ where $B = B(x_1, x_2)$ is a fixed field of bivectors that satisfies for each (x_1, x_2) of Ω the conditions (44) or (46), i.e $B_i(x_1, x_2) = e_i(x_1, x_2)f_i(x_1, x_2)$, the vectors $e_i(x_1, x_2)$ and $f_i(x_1, x_2)$ being orthonormal.

Before to give the precise definition, let us make an important remark. As we want to define an invertible transform, this one has to preserve the fibered structure we have introduced. This means that we need to distinguish (x_1, x_2) as the variable of the image (or of the corresponding section) and (x_1, x_2) as the position of the fiber. To do this we introduce

$$\begin{aligned} \tilde{\sigma}(x_1, x_2, y_1, y_2) &= \\ \sum_i \delta_i(y_1, y_2) e_i(x_1, x_2) &+ \sum_i \tau_i(y_1, y_2) f_i(x_1, x_2) \end{aligned} \quad (61)$$

where

$$\delta_i(y_1, y_2) = \sigma(y_1, y_2) \cdot e_i(y_1, y_2) \quad (62)$$

and

$$\tau_i(y_1, y_2) = \sigma(y_1, y_2) \cdot f_i(y_1, y_2) \quad (63)$$

Definition 1 (Spinor Fourier transform): with the previous notations, the spinor Fourier transform of $\sigma = \sigma(y_1, y_2)$ is given by

$$\mathcal{F}_B \sigma(A) =$$

$$\int_{\mathbb{R}^2} \tilde{\sigma}(x_1, x_2, y_1, y_2) \perp \chi_{A, B(x_1, x_2)}(-y_1, -y_2) dy_1 dy_2 \quad (64)$$

where $B_1 = B_1(x_1, x_2)$ is given by (51). Note that we do not integrate the bivector field B in formula (64).

Let us make explicit the computation for a grey level image. We have:

$$\begin{aligned} \mathcal{F}_B \sigma(u_1, v_1, u_2, v_2) = & \int_{\mathbb{R}^2} e^{-(u_1 y_1 + v_1 y_2) B_1(x_1, x_2)} [\delta_1(y_1, y_2) e_1(x_1, x_2) + \\ & \tau_1(y_1, y_2) f_1(x_1, x_2)] dy_1 dy_2 + \\ & \int_{\mathbb{R}^2} e^{-(u_2 y_1 + v_2 y_2) B_2(x_1, x_2)} [\delta_2(y_1, y_2) e_2(x_1, x_2) + \\ & \tau_2(y_1, y_2) f_2(x_1, x_2)] dy_1 dy_2 \end{aligned} \quad (65)$$

Each one of the integrals

$$\int_{\mathbb{R}^2} e^{-(u_i y_1 + v_i y_2) B_i(x_1, x_2)} [\delta_i(y_1, y_2) e_i(x_1, x_2) + \tau_i(y_1, y_2) f_i(x_1, x_2)] dy_1 dy_2 \quad (66)$$

for $i = 1, 2$, can be identified with

$$\int_{\mathbb{R}^2} e^{-(u_i y_1 + v_i y_2) \sqrt{-1}} [\delta_i(y_1, y_2) + \sqrt{-1} \tau_i(y_1, y_2)] dy_1 dy_2 \quad (67)$$

so that the result of the integration doesn't depend on (x_1, x_2) (recall that $B_i(x_1, x_2)^2 = -1$). The formula (65) can be written as

$$\begin{aligned} \mathcal{F}_B \sigma(u_1, v_1, u_2, v_2) = & \int_{\mathbb{R}^2} e^{-(u_1 y_1 + v_1 y_2) B_1(x_1, x_2)} f_{B_1(x_1, x_2)}(y_1, y_2) dy_1 dy_2 + \\ & \int_{\mathbb{R}^2} e^{-(u_2 y_1 + v_2 y_2) B_2(x_1, x_2)} f_{B_2(x_1, x_2)}(y_1, y_2) dy_1 dy_2 \end{aligned} \quad (68)$$

where, for $i = 1, 2$,

$$f_{B_i(x_1, x_2)}(y_1, y_2) = \delta_i(y_1, y_2) e_i(x_1, x_2) + \tau_i(y_1, y_2) f_i(x_1, x_2) \quad (69)$$

is the projection of the section on the $B_i(x_1, x_2)$ -plane.

Remarks.

- 1) The computation above shows that the spinor Fourier transform is invertible. More precisely:

$$\begin{aligned} \sigma(y_1, y_2) = & \int_{\mathbb{R}^2} e^{(u_1 y_1 + v_1 y_2) B_1(x_1, x_2)} \mathcal{F}_{B_1}(f_{B_1})(u_1, v_1) du_1 dv_1 + \\ & \int_{\mathbb{R}^2} e^{(u_2 y_1 + v_2 y_2) B_2(x_1, x_2)} \mathcal{F}_{B_2}(f_{B_2})(u_2, v_2) du_2 dv_2 \end{aligned} \quad (70)$$

where

$$\begin{aligned} \mathcal{F}_{B_i}(f_{B_i})(u_i, v_i) = & \int_{\mathbb{R}^2} e^{-(u_i y_1 + v_i y_2) B_i(x_1, x_2)} f_{B_i(x_1, x_2)}(y_1, y_2) dy_1 dy_2 \end{aligned} \quad (71)$$

for $i = 1, 2$.

- 2) The formula (67) shows also that the spinor Fourier transform can be computed using usual complex fast Fourier transforms.

- 3) The computations necessitate to introduce first an orthonormal frame field adapted to the B_1 and B_2 -planes, which is denoted $(\nu_{11}, \nu_{12}, \nu_{21}, \nu_{22})$ in the algorithm of Sec. IV. This is done using Gram-Schmidt algorithm starting with the vectors φ_{x_1} and φ_{x_2} .

The procedure is the same for a color image.

IV. SPINOR FOURIER TRANSFORM AND SCALE SPACE

WE begin this section by discussing the links between the previously defined spinor Fourier transform and the scale space of the heat equation. Then, we deal with low-pass filtering interpreted as diffusion for both grey-level and color images.

A. Spinor Fourier transform and diffusion

Let σ_0 be a section corresponding to a grey-level image and $(\nu_{11}, \nu_{12}, \nu_{21}, \nu_{22})$ be the frame field adapted to B_1 and $B_2 = I_4 B_1$ where B_1 encodes the tangent plane of the image surface. Let also H be the Euclidean Laplacian in this frame field. We denote Δ_{B_1} , resp. Δ_{B_2} , the restriction of H to the B_1 -plane, resp. B_2 -plane, and f_{0, B_1} , resp. f_{0, B_2} , the corresponding projections of σ_0 . The solutions of the couple of PDEs

$$\frac{\partial f_{B_1}}{\partial t_1} = \Delta_{B_1} f_{B_1}, \quad f_{B_1}|_{t_1=0} = f_{0, B_1} \quad (72)$$

$$\frac{\partial f_{B_2}}{\partial t_2} = \Delta_{B_2} f_{B_2}, \quad f_{B_2}|_{t_2=0} = f_{0, B_2} \quad (73)$$

are given by

$$f_{B_1}(\cdot, \cdot, t_1) = f_{0, B_1} * K_{t_1} \quad (74)$$

$$f_{B_2}(\cdot, \cdot, t_2) = f_{0, B_2} * K_{t_2} \quad (75)$$

where K_{t_i} , $i = 1, 2$, denote the Gaussian kernels. This means that the solution of the above system of PDEs is

$$f(\cdot, \cdot, t_1, t_2) = \mathcal{F}_B^{-1}(\mathcal{F}_{B_1} f_0 \times \mathcal{F} K_{t_1} + \mathcal{F}_{B_2} f_0 \times \mathcal{F} K_{t_2}) \quad (76)$$

The solution of the PDE

$$\frac{\partial \sigma}{\partial t} = H \sigma, \quad \sigma|_{t=0} = \sigma_0 \quad (77)$$

reads

$$\sigma(\cdot, \cdot, t) = \mathcal{F}_B^{-1}(\mathcal{F}_B \sigma_0 \times \mathcal{F} K_t) \quad (78)$$

that coincides with the restriction on the diagonal $t_1 = t_2$ of the solution (76).

In the case of color images, the system splits into three PDEs since the embedding space is of dimension 6.

B. Experiments

The algorithm (for grey-level image) is the following one:

- 1) Compute the bivector B_1 encoding the tangent plane (formula (51)).
- 2) Construct an orthonormal frame field $(\nu_{11}, \nu_{12}, \nu_{21}, \nu_{22})$ adapted to the B_1 -plane and the $B_2 = I_4 B_1$ -plane.
- 3) Compute the expression of the section σ in the frame field $(\nu_{11}, \nu_{12}, \nu_{21}, \nu_{22})$.
- 4) In the frame field $(\nu_{11}, \nu_{12}, \nu_{21}, \nu_{22})$, the spinor Fourier transform splits into two usual complex Fourier transforms (cf. formula (65)).
- 5) Multiply the Fourier spectra with Gaussians of variance t_1 and t_2 for $t_1, t_2 \in \mathbb{R}$.
- 6) Compute the inverse Fourier transforms.
- 7) Change the frame field $(\nu_{11}, \nu_{12}, \nu_{21}, \nu_{22})$ to the standard one.

We test the algorithm on the grey-level images 'Barbara' (Fig. 1) and 'Lake' (Fig. 2). We first show the projections of the images on the tangent and normal bundles. As expected, the tangent bundle component (top-center images) encodes information about the local variations of the image. Indeed, we observe that the higher is the gradient of the original image, the higher is the grey level of the tangent bundle part. Hence, homogeneous regions are represented in black and strongest contours in white. The normal bundle component (top-right images) corresponds to the original image where the contours have been thickened and darkened. It provides a highlight of the local variations of the original image.

Then, we show the result of the diffusion process along the diagonal at different times ($t = 0.0001$, $t = 0.1$ and $\lim_{t \rightarrow \infty}$). We observe that the diffusion combines two behaviours: an Euclidean heat diffusion and a preservation of the contours. The first behaviour comes from the fact that the differential operator involved in the PDE is the Euclidean Laplacian (in a moving frame) and the diffusion process does not affect the moving frame. The second behaviour might be explained by the chosen moving frame that encodes the local variations of the image. When $t \rightarrow \infty$ (bottom-right images), the result is the superposition of the contours on the mean grey level of the image, the latter being the limit when $t \rightarrow \infty$ of the Euclidean heat diffusion.

The algorithm above might be extended in a straightforward way to color images. We test this algorithm on the color versions of the image 'Barbara' (Fig. 3) and 'Lake' (Fig. 4). As for the case of grey-level images, the tangent bundle component (top-center images) encodes information about the local variations of the image. Whereas homogeneous regions still appear in black, the contours are now colored; the interpretation here is more complicated than in the case of grey-level images since the color of the contour depend not only of magnitude of the color variation but also of the colors making the contour in the original image. The normal bundle component (top-right image) still provides a highlight of the local variations of the original image.

We perform the diffusion process and show results along the

diagonal at the times ($t = 0.0001$, $t = 0.1$ and $\lim_{t \rightarrow \infty}$). The diffusion combines two behaviours: a marginal Euclidean heat diffusion and a preservation of the contours. When $t \rightarrow \infty$ (bottom-right images), the result is the superposition of the contours on the mean color of the image, the latter being the limit when $t \rightarrow \infty$ of the marginal Euclidean heat diffusion. Finally, the experiments on color images confirm that our approach is non marginal since the contours (computed in a non marginal way) are preserved all along the diffusion process.

V. CONCLUSION

We have shown in this paper how to define a spinor Fourier transform that allows to analyze frequencies of grey-level or color images taking into account the geometric data of the corresponding image surfaces. When dealing with color images, this new defined transform treats all the colorimetric information in a really non marginal way.

The construction involves group actions via spin characters, these ones being parametrized by bivectors of the Clifford algebra. A natural choice for the bivectors is the one corresponding to the tangent planes of the image surface. But other bivectors can be considered.

We have proposed applications to low-pass filtering interpreted as diffusion process with heat equation. Other types of filtering can be envisaged. One may also consider applications for instance to color image compression, deblurring or to generalized color Fourier descriptors (as in [24]).

In this work, we have only treated the case of standard representations of the spin groups. As mentioned before there exist other representations called spin representations that do not descend to the orthogonal groups. Dealing with these representations necessitates to introduce complex representations of Clifford algebras. This will be the subject of a forthcoming paper.

APPENDIX A

CLIFFORD ALGEBRAS AND SPIN GROUPS

We only give here the basic notions used throughout the text, more details can be found for instance in [9]. We denote $\mathbb{R}_{p,q}$ the Clifford algebra of the vector space \mathbb{R}^n equipped with the non degenerate quadratic form $Q_{p,q}$ of signature (p, q) . Let us mention that $\mathbb{R}_{0,1}$ is isomorphic to \mathbb{C} and $\mathbb{R}_{0,2}$ is isomorphic to the algebra \mathbb{H} of quaternions.

The group $Spin(n)$ of the Clifford algebra $\mathbb{R}_{n,0}$ is defined by

$$Spin(n) = \{\tau \in \mathbb{R}_{n,0}, \alpha(\tau) = \tau, \tau\tau^\dagger = 1, \tau u \tau^{-1} \in \mathbb{R}^n \forall u \in \mathbb{R}^n\} \quad (79)$$

where α is the main involution and \dagger is the reversion of $\mathbb{R}_{n,0}$. We denote

$$u \perp \tau := \tau u \tau^{-1} \quad (80)$$

the action of $Spin(n)$ on \mathbb{R}^n . The map

$$\rho_n : Spin(n) \longrightarrow SO(n, \mathbb{R}) \quad (81)$$

defined by $\rho_n(\tau)(u) = u \perp \tau$ is an onto group morphism with kernel \mathbb{Z}_2 . It is the standard representation of $Spin(n)$.

It can be checked that $Spin(2)$ is isomorphic to \mathbb{S}^1 (\mathbb{S}^1 is the group of unit complex numbers), $Spin(3)$ is isomorphic to \mathbb{H}^1 (\mathbb{H}^1 is the group of unit quaternions) and $Spin(4)$ is isomorphic to $\mathbb{H}^1 \times \mathbb{H}^1$. It is well known that $Spin(n)$ is a compact connected Lie group of dimension $n(n-1)/2$. The Lie algebra $\mathfrak{spin}(n)$ of $Spin(n)$ is the vector space of bivectors of $\mathbb{R}_{n,0}$, denoted $\mathbb{R}_{n,0}^2$, with the Lie bracket given by the commutator. Since the exponential map is onto (see [19]), every element τ of $Spin(n)$ can be written as

$$\tau = \sum_{i \geq 0} \frac{1}{i!} B^i \quad (82)$$

for some B in $\mathbb{R}_{n,0}^2$.

Hestenes algorithm (see [20]) states that every bivector B of $\mathbb{R}_{n,0}^2$ can be written as

$$B = B_1 + B_2 + \dots + B_m \quad (83)$$

where $m \leq n/2$, $B_j = \|B_j\| a_j b_j$ for j in $\{1, 2, \dots, m\}$, and $\{a_1, \dots, a_m, b_1, \dots, b_m\}$ is a set of orthonormal vectors of \mathbb{R}^n . Thus,

$$B_j B_k = B_k B_j = B_k \wedge B_j \quad (84)$$

for $j \neq k$ and

$$B_k^2 = -\|B_k\|^2 < 0 \quad (85)$$

This means that the B_j -planes are orthogonal and implies

$$e^{B_1 + \dots + B_m} = e^{B_{\sigma(1)}} \dots e^{B_{\sigma(m)}} \quad (86)$$

for all permutation σ . Since B_j^2 is negative, we have

$$e^{B_j} = \cos(\|B_j\|) + \frac{\sin(\|B_j\|) B_j}{\|B_j\|} \quad (87)$$

The corresponding rotation

$$R_{B_j} : u \mapsto e^{-B_j} u e^{B_j} = u \perp e^{B_j} \quad (88)$$

acts in the oriented B_j -plane as a plane rotation of angle $2\|B_j\|$. The vectors orthogonal to B_j are invariant under R_{B_j} .

APPENDIX B

ABSTRACT FOURIER TRANSFORM

Let G be a locally compact unimodular group. The Pontryagin dual of G , denoted \hat{G} , is the set of equivalent classes of unitary irreducible representations of G . The Fourier transform of a function f of $L^2(G, \mathbb{C})$ is defined on \hat{G} by

$$\mathcal{F}(f)(\varphi) = \int_G f(g) \varphi(g^{-1}) d\nu(g) \quad (89)$$

where ν is a Haar measure on G .

It appears that when G is abelian, every irreducible representation of G is of dimension 1. Such a unitary representation is thus a group morphism from G to \mathbb{S}^1 and is called a character of G . As an example, let us mention that the Pontryagin dual \mathbb{R}^n of the additive group \mathbb{R}^n is \mathbb{R}^n itself and that the corresponding Fourier transform, given by formula (89), is the usual Fourier transform on \mathbb{R}^n . Dealing with the rotation group $SO(2, \mathbb{R})$ leads to the theory of Fourier series (the Pontryagin dual is \mathbb{Z}) and dealing with the finite group $\mathbb{Z}/N\mathbb{Z}$ leads to the definition of the discrete Fourier transform (the Pontryagin dual is $\mathbb{Z}/N\mathbb{Z}$).

REFERENCES

- [1] T. Batard, M. Berthier and C. Saint Jean: *Clifford Fourier Transform for Color Image Processing*. In Geometric Algebra Computing for Engineering and Computer Science. E. Bayro Corrochano and G. Scheuermann Eds, Springer, 2010, pp.135-162.
- [2] T. Batard, C. Saint Jean and M. Berthier: *A Metric Approach to nD Images Edge Detection with Clifford Algebras*. J Math Imaging Vis, 2009, vol. 33, pp. 296-312.
- [3] F. Brackx, N. De Schepper and F. Sommen: *The Two Dimensional Clifford Fourier Transform*. J Math Imaging Vis, 2006, vol. 26, pp. 5-18.
- [4] F. Brackx, N. De Schepper and F. Sommen: *The Fourier transform in Clifford analysis*. Adv. Imag. Elect. Phys. 156 (2008), pp. 55-203.
- [5] R. Bujack, G. Scheuermann and E. Hitzer: *A general geometric Fourier transform*. In 9th Int. Conf. on Clifford Algebras and their Applications in Mathematical Physics. K. Gürlebeck (ed.). Weimar, Germany, 15-20 July 2011. 19 pages.
- [6] R. Bujack, G. Scheuermann and E. Hitzer: *A general geometric Fourier transform convolution theorem*. To appear in Adv. Appl. Clifford Alg.
- [7] T. Bülw: *Hypercomplex Spectral Signal Representation for the Processing and Analysis of Images*. Ph.D Thesis, Kiel, 1999.
- [8] T. Bülw and G. Sommer: *Hypercomplex signals - a novel extension of the analytic signal to the multidimensional case*. IEEE Transactions on Signal Processing, 2001, Vol. 49, 11, pp. 2844-2852.
- [9] C. Chevalley: *The Algebraic Theory of Spinors and Clifford Algebras*. Springer, New Edn., 1995.
- [10] S. Dahlke, G. Kutyniok, G. Steidl and G. Teschke: *Shearlet Coorbit Spaces and Associated Banach Frames*. Appl. Comput. Harmon. Anal. 27 (2009) pp. 195-214.
- [11] H. De Bie: *Clifford algebras, Fourier transforms and quantum mechanics*. To appear in Math. Methods Appl. Sci.
- [12] H. De Bie and Y. Xu: *On the Clifford Fourier transform*. Int. Math. Res. Not. IMRN, 2011, No. 22, pp. 5123-5163.
- [13] G. Demarcq, L. Mascarilla, M. Berthier and P. Courtellement: *The Color Monogenic Signal. Application to Color Edge Detection and Color Optical Flow*. J Math Imaging Vis, 2011, vol. 40, pp. 269-284.
- [14] J. Ebling and G. Scheuermann: *Clifford Fourier Transform on Vector Fields*. IEEE Transactions on Visualization and Computer Graphics, 2001, vol. 49 (11), pp. 2844-2852.
- [15] T. A. Ell and S. Sangwine: *Hypercomplex Fourier Transforms of Color Images*. IEEE Transactions on Image Processing, 2007, Vol. 16, 1, pp. 22-35.
- [16] M. Felsberg: *Low-level Image Processing with the Structure Multivector*. Ph.D Thesis, Kiel, 2002.
- [17] M. Felsberg and G. Sommer: *The Monogenic Signal*. IEEE Transactions on Signal Processing, 2001, vol. 49 (12), pp. 3136-3144.
- [18] T. Frankel: *The Geometry of Physics - An Introduction*. Revised Edition, Cambridge University Press.
- [19] S. Helgason: *Differential Geometry, Lie Groups and Symmetric Spaces*. Academic Press, London, 1978.
- [20] D. Hestenes and G. Sobczyk: *Clifford Algebra to Geometric Calculus*. Reidel, Dordrecht, 1984.
- [21] H.B. Lawson and M.-L. Michelsohn: *Spin Geometry*. Princeton University Press, Princeton, New Jersey, 1989.
- [22] P. Lounesto: *Clifford Algebras and Spinors*. Second Edition, London Mathematical Society Lecture Note Series 286, Cambridge University Press, 2001.
- [23] R. Lukac, K. N. Plataniotis, B. Smolka and A. N. Venetsanopoulos: *Vector Operators for Color Image Zooming*. IEEE Int. Symp. on Industrial Electronics, 2005.
- [24] J. Mennesson, C. Saint Jean and L. Mascarilla: *New Geometric Fourier Descriptors for Color Image Recognition*. IEEE Int. Conf. on Image Processing, 2010.
- [25] M. Postnikov: *Leçons de géométrie : groupes et algèbres de Lie*. MIR, 1985.
- [26] S. Sangwine and T.A. Ell: *Hypercomplex Fourier Transform of Color Images*. IEEE Int. Conf. on Image Processing, 2001, vol. 1, pp. 137-140.
- [27] F. Smach, C. Lemaire, J.-P. Gauthier, J. Miteran and M. Atri: *Generalized Fourier Descriptors with Applications to Objects Recognition in SVM Context*. J Math Imaging Vis, 2008, vol. 30 (1), pp. 43-71.
- [28] N.J. Vilenkin: *Special Functions and the Theory of Group Representations*. Translations of Mathematical Monographs, vol. 22. American Mathematical Society, Providence, Rhode Island (1968).



Fig. 1. Top: Grey-level image 'Barbara' (Left) and its projection on the tangent bundle (Center) and the normal bundle (Right). Bottom: Diffusion of the Image 'Barbara' at the times $t = 0.0001$ (Left), $t = 0.01$ (Center) and $\lim_{t \rightarrow \infty}$ (Right).



Fig. 2. Top: Grey-level image 'Lake' (Left) and its projection on the tangent bundle (Center) and the normal bundle (Right). Bottom: Diffusion of the Image 'Lake' at the times $t = 0.0001$ (Left), $t = 0.01$ (Center) and $\lim_{t \rightarrow \infty}$ (Right).

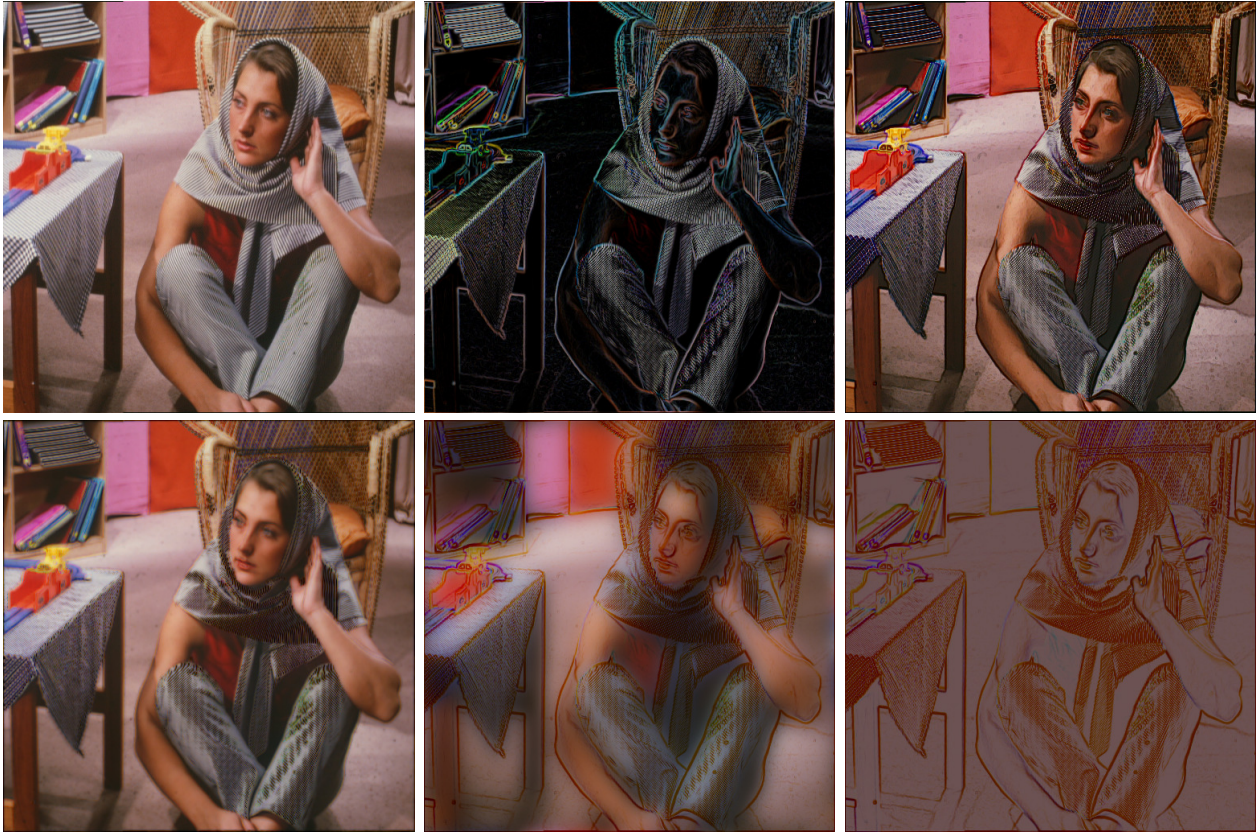


Fig. 3. Top: Color image 'Barbara' (Left) and its projection on the tangent bundle (Center) and the normal bundle (Right). Bottom: Diffusion of the Image 'Barbara' at the times $t = 0.0001$ (Left), $t = 0.01$ (Center) and $\lim_{t \rightarrow \infty}$ (Right).

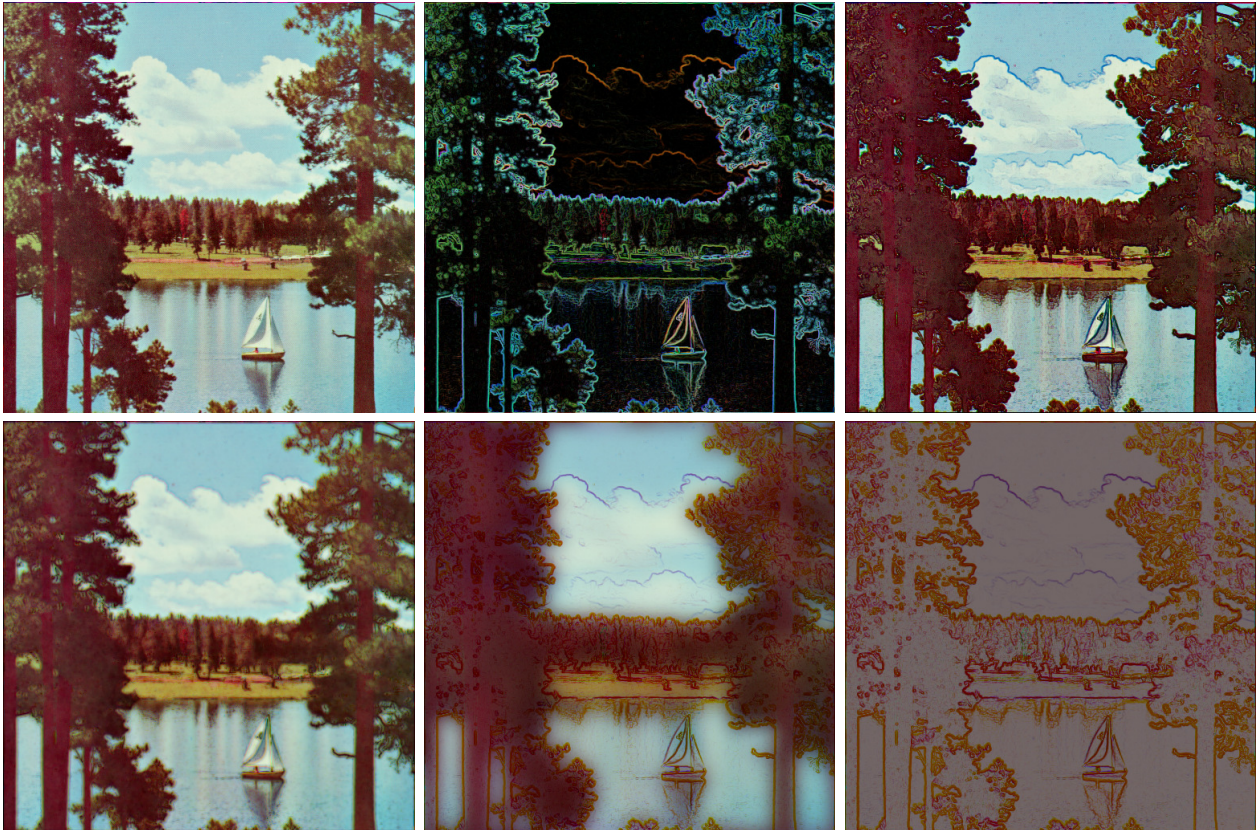


Fig. 4. Top: Color image 'Lake' (Left) and its projection on the tangent bundle (Center) and the normal bundle (Right). Bottom: Diffusion of the Image 'Lake' at the times $t = 0.0001$ (Left), $t = 0.01$ (Center) and $\lim_{t \rightarrow \infty}$ (Right).